

Electronic Supplementary Material (ESI) for Journal of Materials Chemistry C.

This journal is © The Royal Society of Chemistry 2017

Triphenothiazinyl triazacoronenes: Donor–acceptor molecular graphene exhibiting multiple fluorescence and electrogenerated chemiluminescence emissions

Ying Zhao,^a Qiang Zhang,^a Ke Chen,^a Hongfang Gao,^a Honglan Qi,^{†a} Xianying Shi,^a Yajun Han,^a Junfa Wei,^{†a} Chengxiao Zhang^{†a}

Key Laboratory of Applied Surface and Colloid Chemistry (Ministry of Education), School of Chemistry and Chemical Engineering, Shaanxi Normal University, Xi'an, 710062, P.R. China.

† Corresponding Authors: cxzhang@snnu.edu.cn; weijf@snnu.edu.cn; honglanqi@snnu.edu.cn.

Table of Contents

Figure S1	¹ H NMR spectrum of TPTZ-TAC1 recorded in CDCl ₃	S3
Figure S2	¹³ C NMR spectrum of TPTZ-TAC1 recorded in CDCl ₃	S3
Figure S3	HRMS (ESI) spectrum of TPTZ-TAC1 recorded in THF/CH ₃ CN	S4
Figure S4	Photo of PTZ, TAC and TPTZ-TAC1	S4
Figure S5	Photo of different concentrations of TPTZ-TAC1	S5
Figure S6	Absorption spectra of TPTZ-TAC1 at different concentrations	S5
Figure S7	Normalized absorption spectra for TPTZ-TAC1 in different solvents	S6
Figure S8	Normalized fluorescence spectra for TPTZ-TAC1 in different solvents	S6
Figure S9	Normalized absorption and fluorescence spectra for TPTZ-TACs	S7
Figure S10	Normalized fluorescence spectra for different concentrations of TPTZ-TACs	S8
Figure S11	Cyclic voltammograms of TPTZ-TAC1	S9
Figure S12	Cyclic voltammograms of TPTZ-TAC1 with different scan rates	S10
Figure S13	Cyclic voltammogram of TPTZ-TAC1 at platinum UME	S11
Figure S14	Plot of the experimental ratio i_t/i_{ss} against the inverse square root of time	S11
Figure S15	Comparison between simulated and experimental oxidation waves for TPTC-TAC1	S12
Figure S16	Comparison between simulated and experimental reduction waves for TPTC-TAC1	S13
Figure S17	Cyclic voltammograms of TPTZ-TAC2 and TPTZ-TAC3	S14
Figure S18	Comparison between simulated and experimental reduction waves for TPTZ-TAC2	S15
Figure S19	Comparison between simulated and experimental reduction waves for TPTZ-TAC3	S16
Figure S20	Comparison between simulated and experimental oxidation waves for TPTZ-TAC2	S17
Figure S21	Comparison between simulated and experimental oxidation waves for TPTZ-TAC3	S18
Figure S22	ECL and CV simultaneous measurements for TPTZ-TAC1	S19
Figure S23	Normalized fluorescence and ECL spectra of TPTZ-TAC1	S20
Figure S24	Normalized fluorescence and ECL spectra of TPTZ-TAC2	S20
Figure S25	Normalized fluorescence and ECL spectra of TPTZ-TAC3	S21

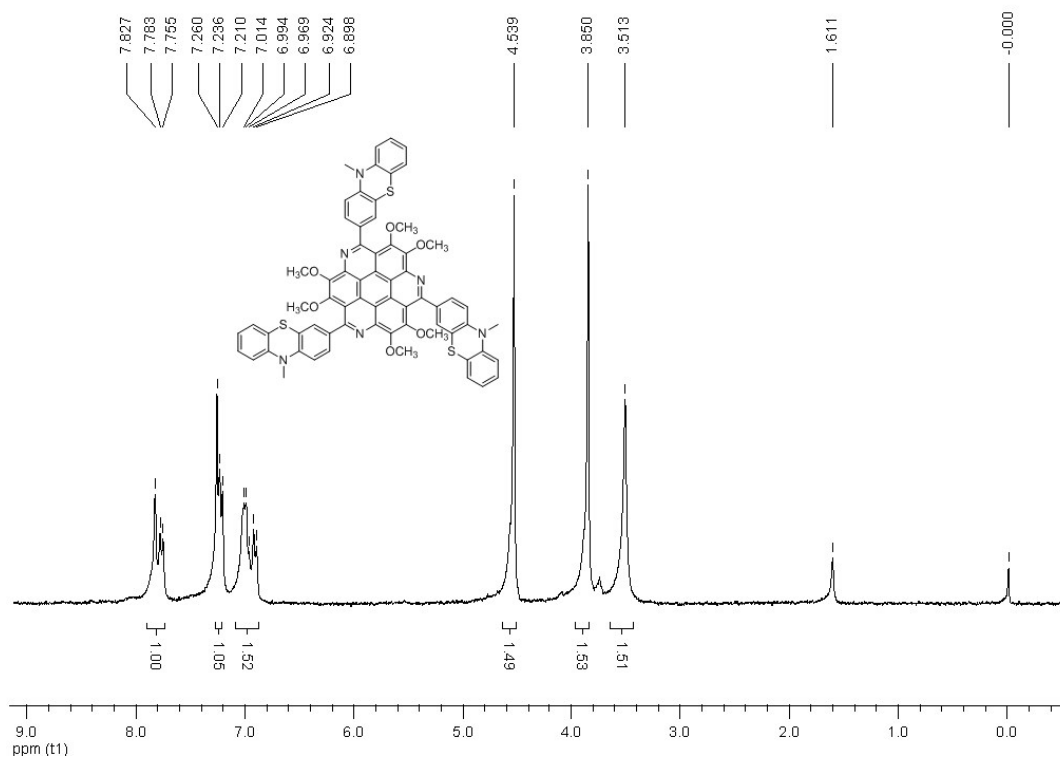


Figure S-1. ¹H NMR spectrum of TPTZ-TAC1 recorded in CDCl₃

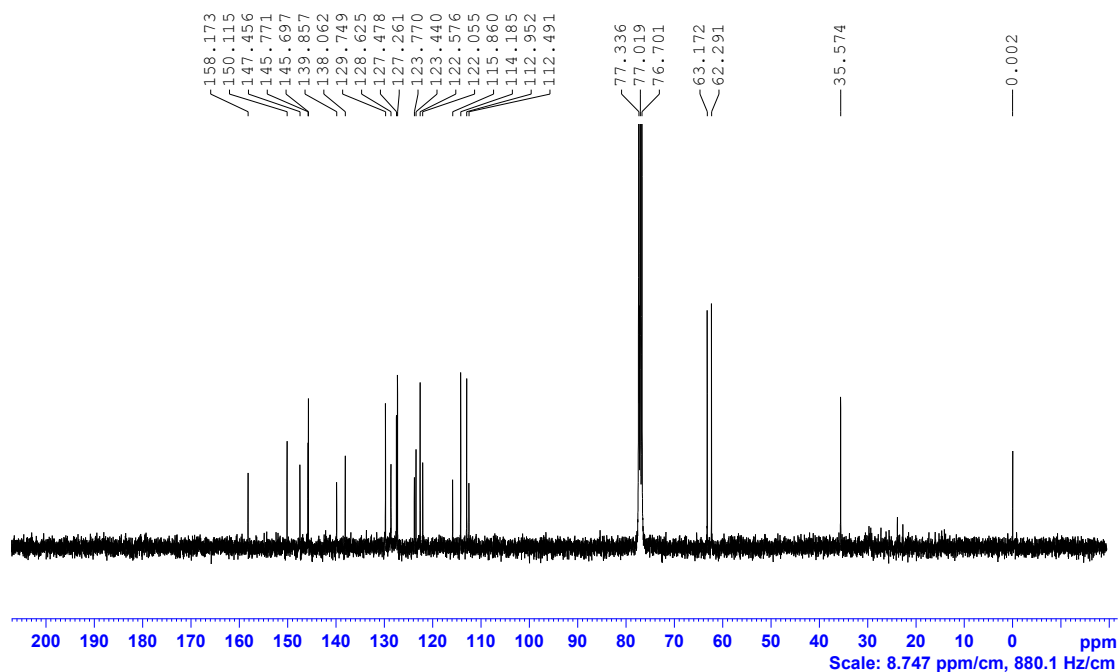


Figure S-2. ¹³C NMR spectrum of TPTZ-TAC1 recorded in CDCl₃

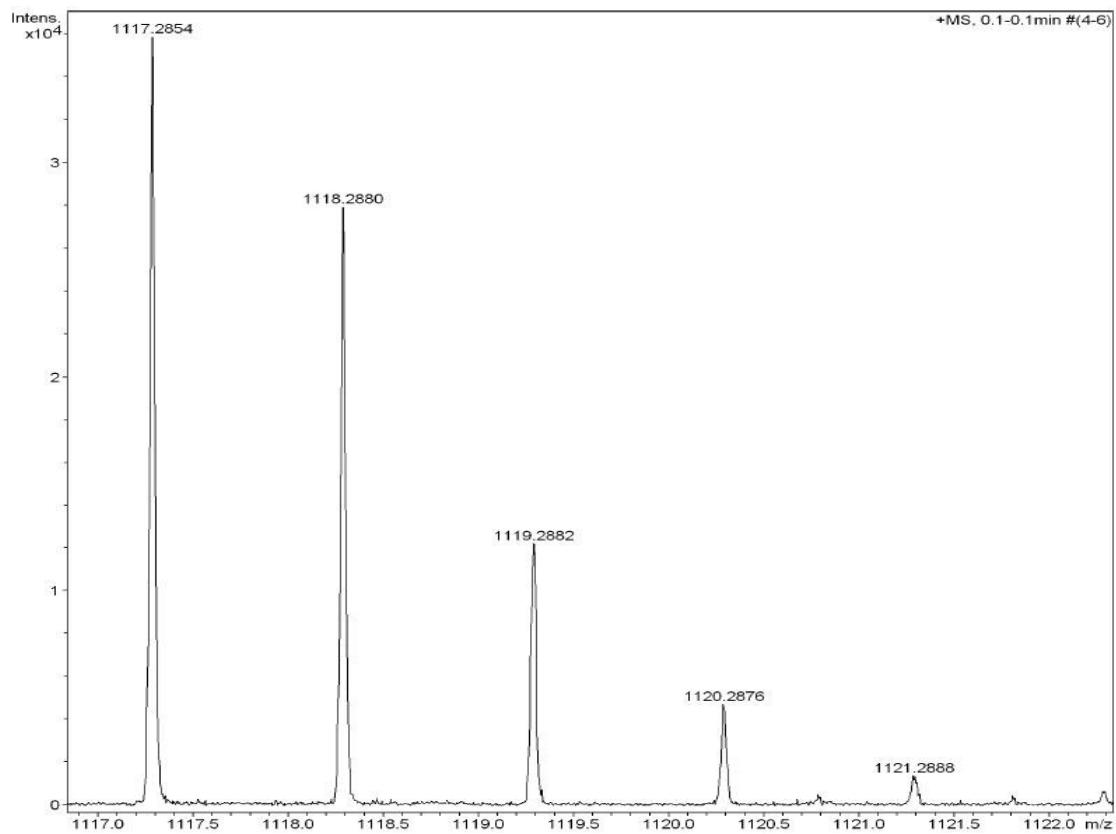


Figure S-3. HRMS (ESI) spectrum of TPTZ-TAC1 recorded in THF/CH₃CN.



Figure S-4. Photo of 1×10^{-5} M PTZ, TAC and TPTZ-TAC1 in benzene: MeCN ($v:v=1:1$) from left to right.

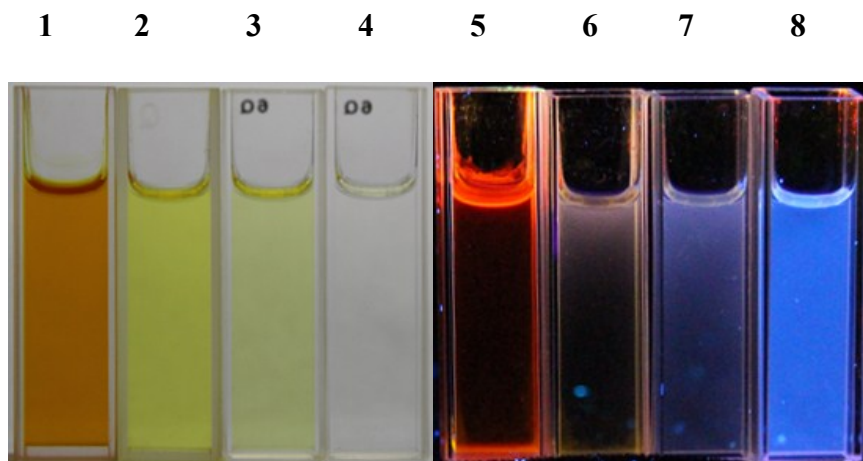


Figure S-5. Photo of 1×10^{-3} M, 2×10^{-5} M, 1×10^{-5} M, 5×10^{-7} M TPTZ-TAC1 in benzene: MeCN ($v:v=1:1$) from left to right. 1-4 in bright light, 5-8 excited in 365 nm UV lamp in dark condition.

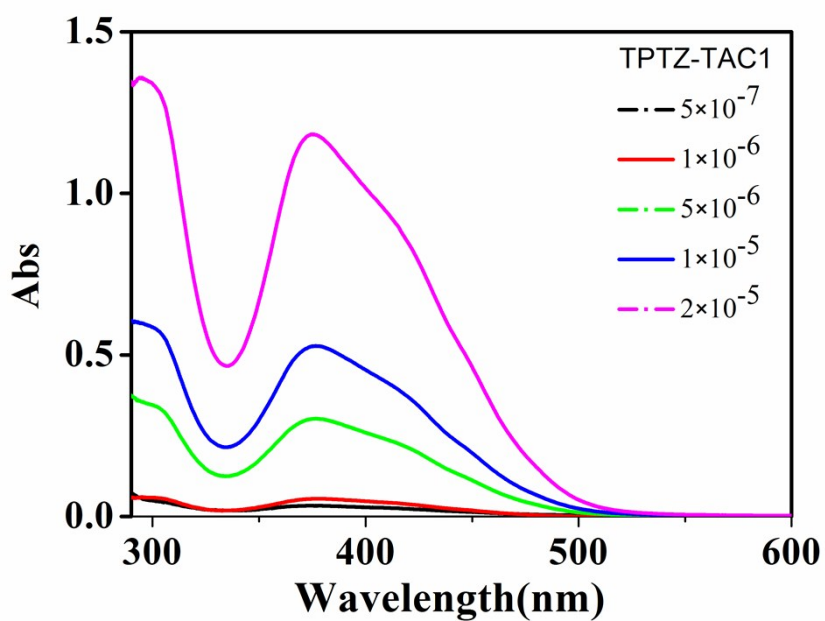


Figure S-6. Absorption spectra of TPTZ-TAC1 at different concentrations in benzene: MeCN ($v:v=1:1$).

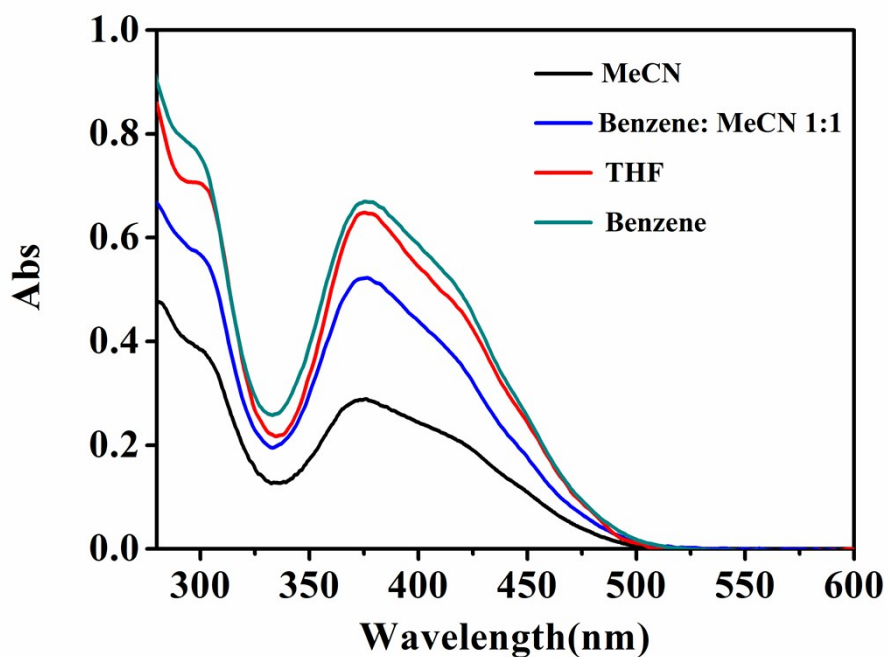


Figure S-7. Absorption spectra of 10 μM TPTZ-TAC1 in different solvents.

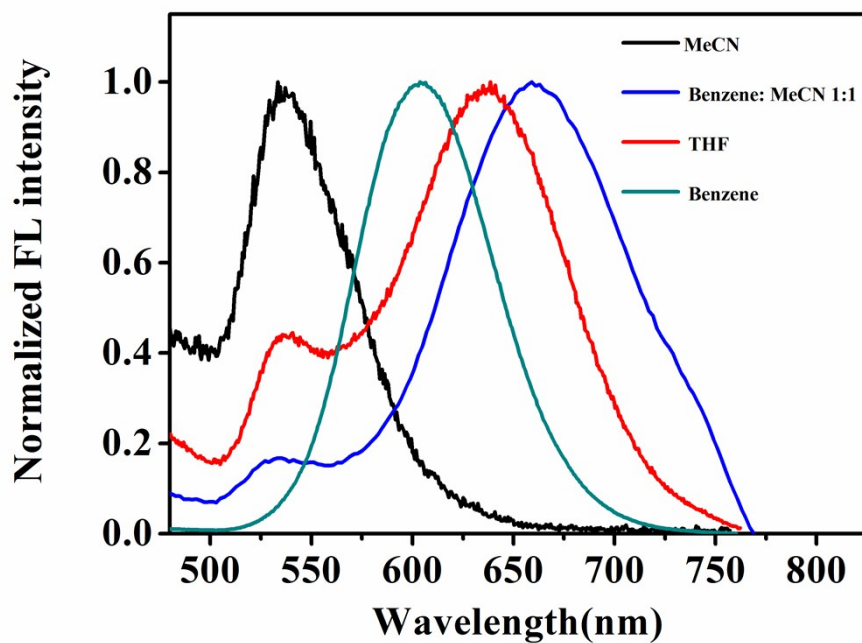


Figure S-8. Normalized fluorescence spectra for 20 μM TPTZ-TAC1 in different solvents.

Fluorescence emissions were excited at the absorption maximum wavelength.

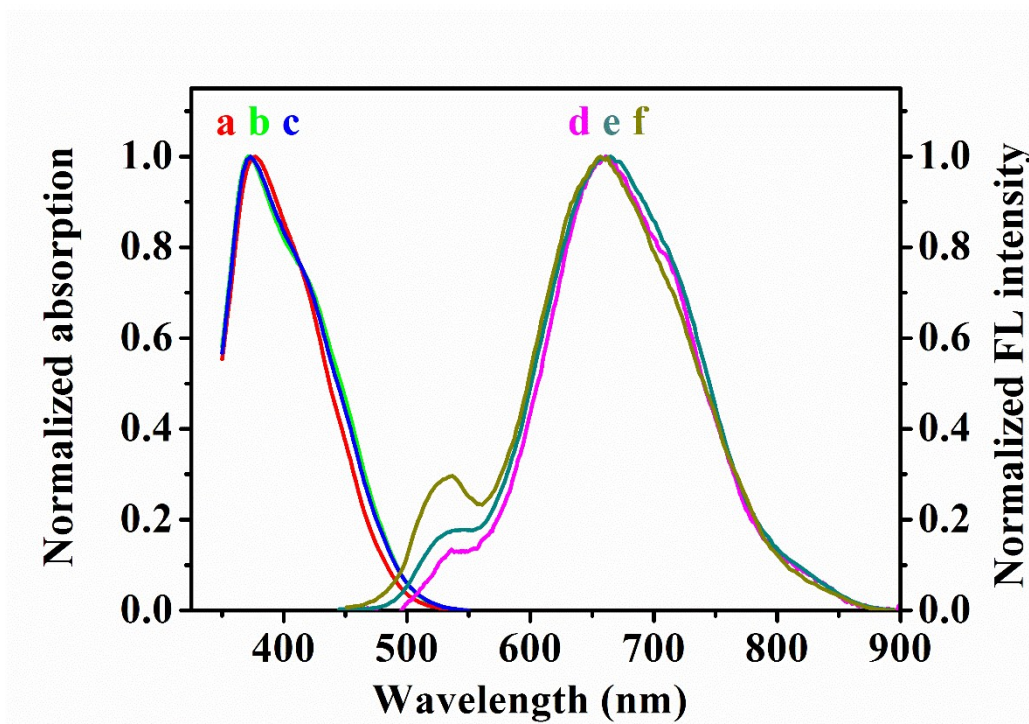


Figure S-9. Normalized absorption (a, b, c) and fluorescence spectra (d, e, f) for 10 μM TPTZ-TAC1 (a, d), 10 μM TPTZ-TAC2 (b, e) and 10 μM TPTZ-TAC3 (c, f) in benzene: MeCN ($v:v=1:1$). Fluorescence emissions were excited at the absorption maximum wavelength.

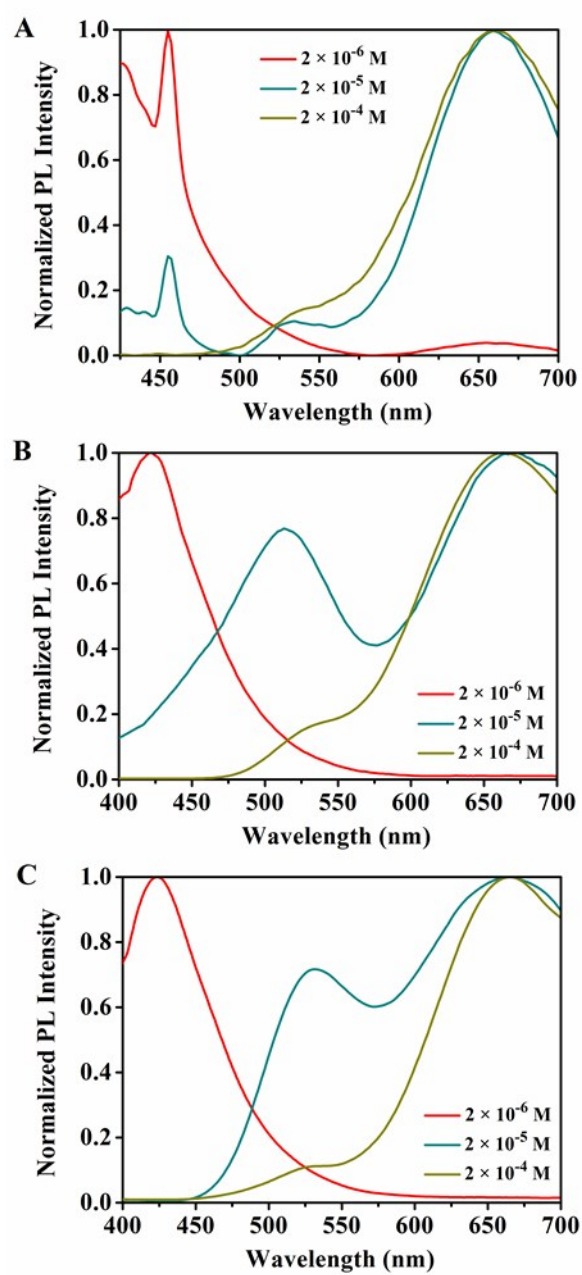


Figure S-10. Normalized fluorescence spectra for different concentrations of TPTZ-TAC1 (A), TPTZ-TAC2 (B) and TPTZ-TAC3 (C) in benzene: MeCN ($v:v=1:1$). Fluorescence emissions were excited at the absorption maximum wavelength.

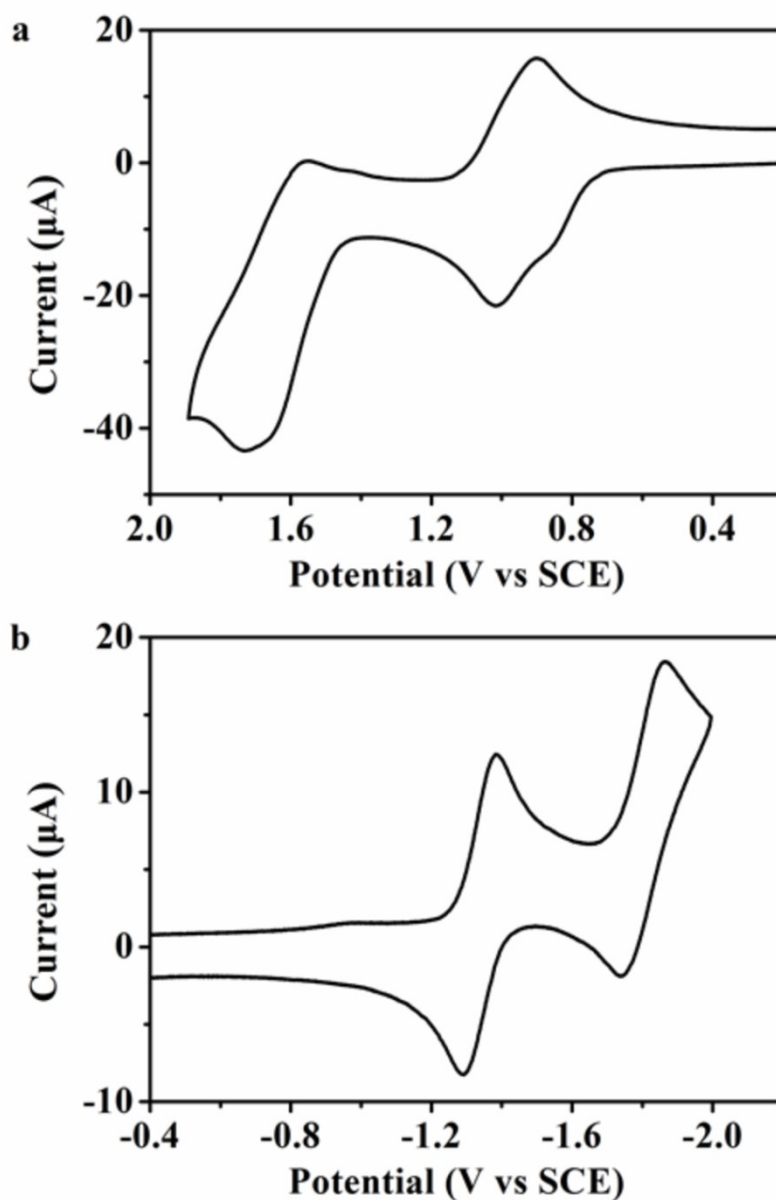


Figure S-11. Cyclic voltammograms of 1.5 mM TPTZ-TAC1 in benzene: MeCN (v:v=1:1) containing 0.1 M TBAPF₆ with a scan rate of 0.5 V/s at a Pt electrode (electrode area is 0.027cm²).

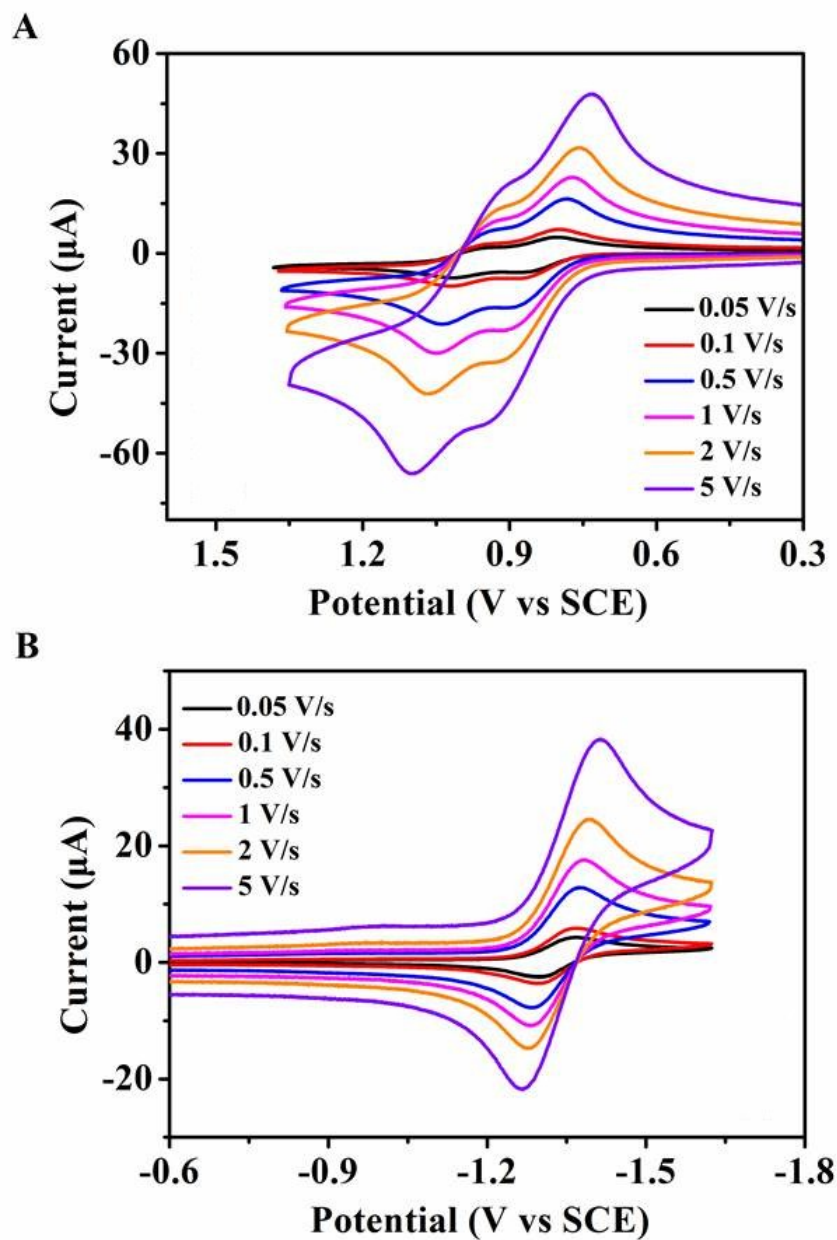


Figure S-12. Cyclic voltammograms of 1.5 mM TPTZ-TAC1 in benzene: MeCN ($v:v=1:1$) containing 0.1 M TBAPF₆ at a Pt electrode (electrode area is 0.027cm²) with different scan rates.

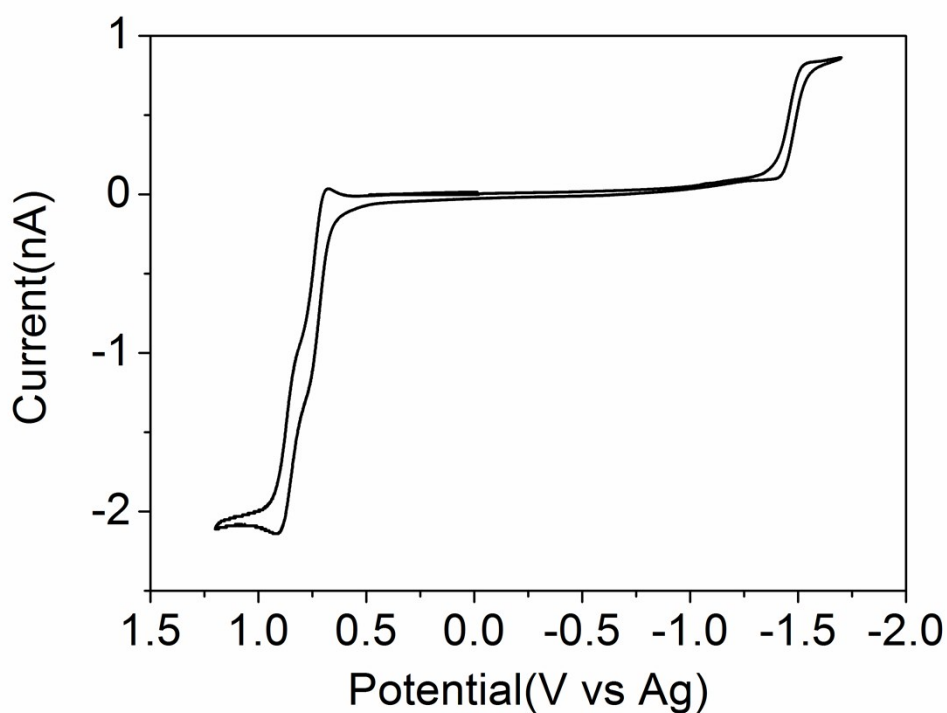


Figure S-13. Cyclic voltammogram of 1.5 mM TPTZ-TAC1 in benzene: MeCN ($v:v=1:1$) containing 0.1M TBAPF₆ at platinum UME ($r = 11 \mu\text{m}$) with a scan rate of 10 mV/s.

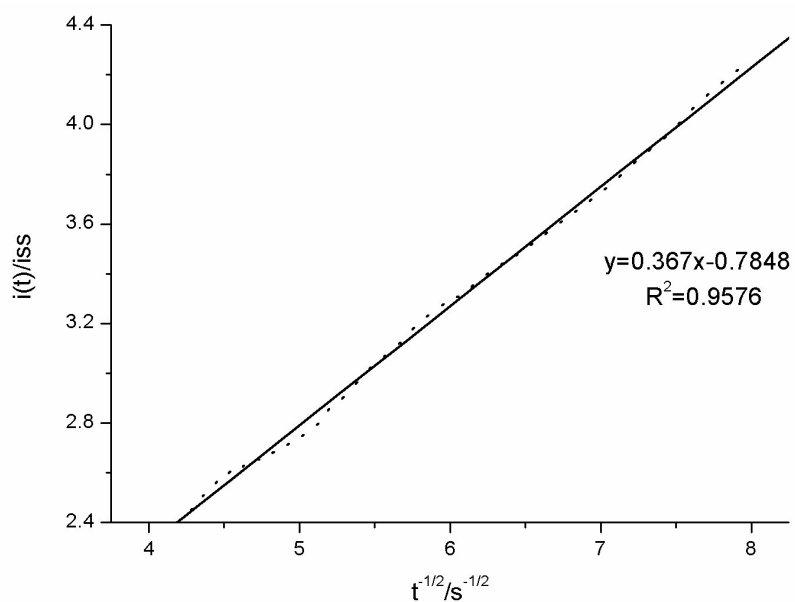


Figure S-14. Plot of the experimental ratio $i(t)/i_{ss}$ against the inverse square root of time (s). The data were obtained in benzene: MeCN ($v:v=1:1$) containing 1.5 mM PTZ-TAC1 and 0.1 M TBAPF₆ at an platinum UME ($r = 11 \mu\text{m}$), and oxidation at $E = +1.1 \text{ V vs Ag}$.

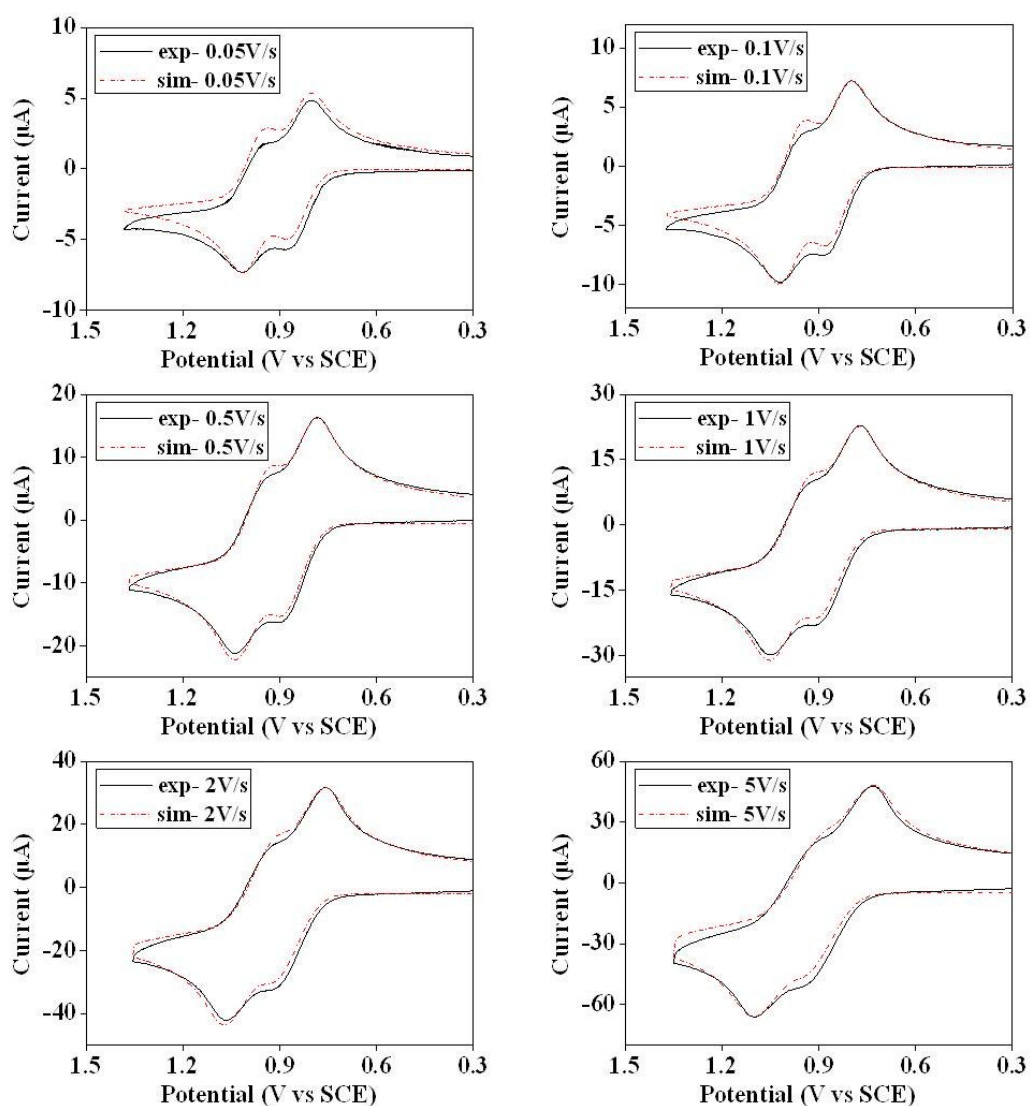


Figure S-15. Comparison between simulated and experimental oxidation waves for 1.5 mM TPTZ-TAC1 at different scan rates. The model for these oxidation simulations: ECE, with $n = 2$, with a heterogeneous rate constant, $\alpha = 0.5$, $k_1^0 = 0.05$ cm/s, $k_2^0 = 0.04$ cm/s. Simulated data: $E_1^0 = 0.84$ V vs SCE, $E_2^0 = 0.96$ V vs SCE; Diffusion coefficient: 7.05×10^{-6} cm²/s, uncompensated resistance 666 Ω , capacitance 1×10^{-6} F. Experimental conditions: solvent: benzene: MeCN ($v:v=1:1$), supporting electrolyte: 0.1 M TBAPF₆, Pt electrode area 0.027 cm².

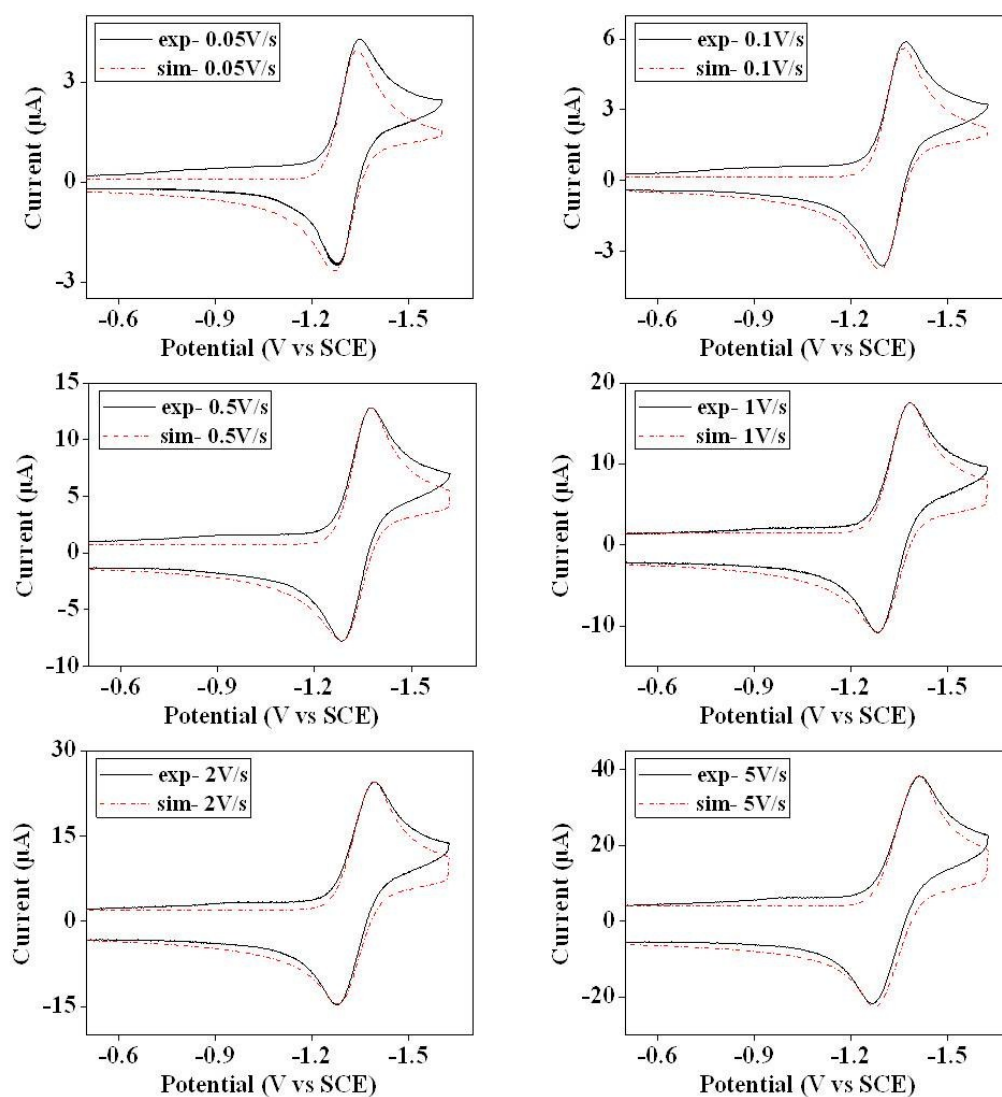


Figure S-16. Comparison between simulated and experimental reduction waves for 1.5 mM TPTZ-TAC1 at different scan rates. The model for these reduction simulations: EC, with $n = 1$, with a heterogeneous rate constant, $\alpha = 0.5$, $k^0 = 1 \times 10^4$ cm/s and a homogeneous forward rate constant, $k_{\text{eq}} = 0.5$, $k_f = 8$ s $^{-1}$. Simulated data: $E^\circ = -1.34$ V vs SCE; Diffusion coefficient: 7.05×10^{-6} cm 2 /s, uncompensated resistance 883 Ω , capacitance 1.5×10^{-6} F. Experimental conditions: solvent: benzene: MeCN ($v:v=1:1$), supporting electrolyte: 0.1 M TBAPF $_6$, Pt electrode area 0.027 cm 2 .

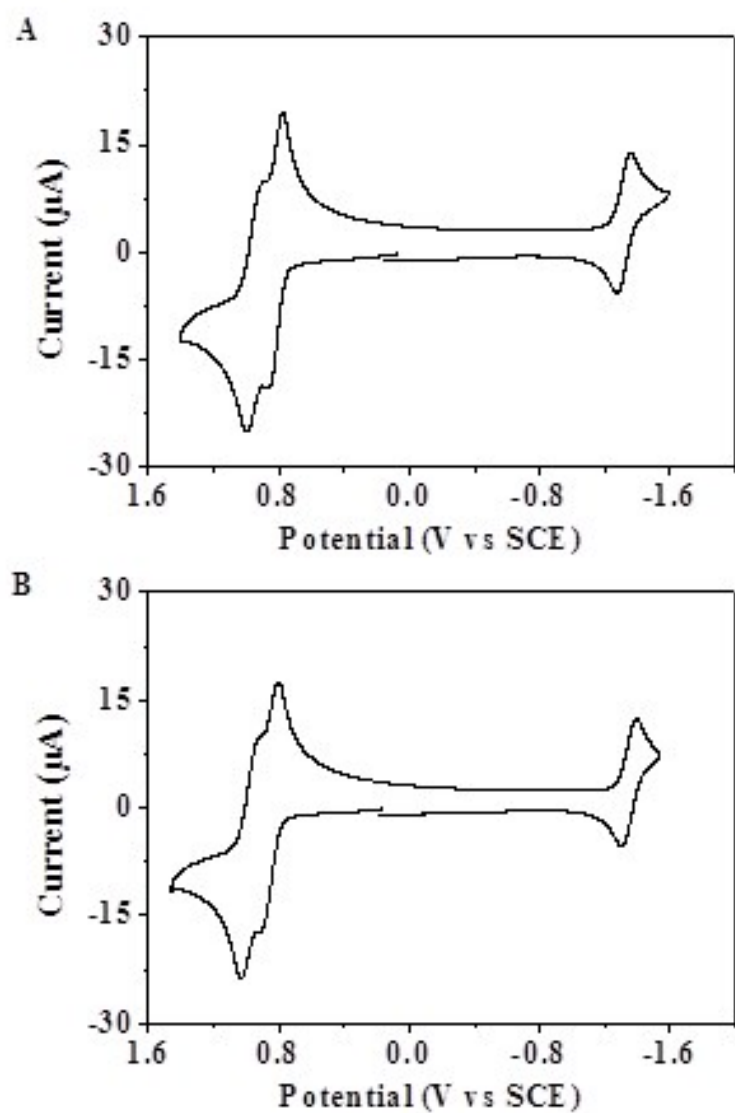


Figure S-17. Cyclic voltammograms of 1.5 mM TPTZ-TAC2 (A) and 1.5 mM TPTZ-TAC3 (B) in benzene: MeCN ($v:v=1:1$) containing 0.1 M TBAPF₆ at platinum electrode with scan rate of 0.5 V/s (electrode area is 0.027 cm²).

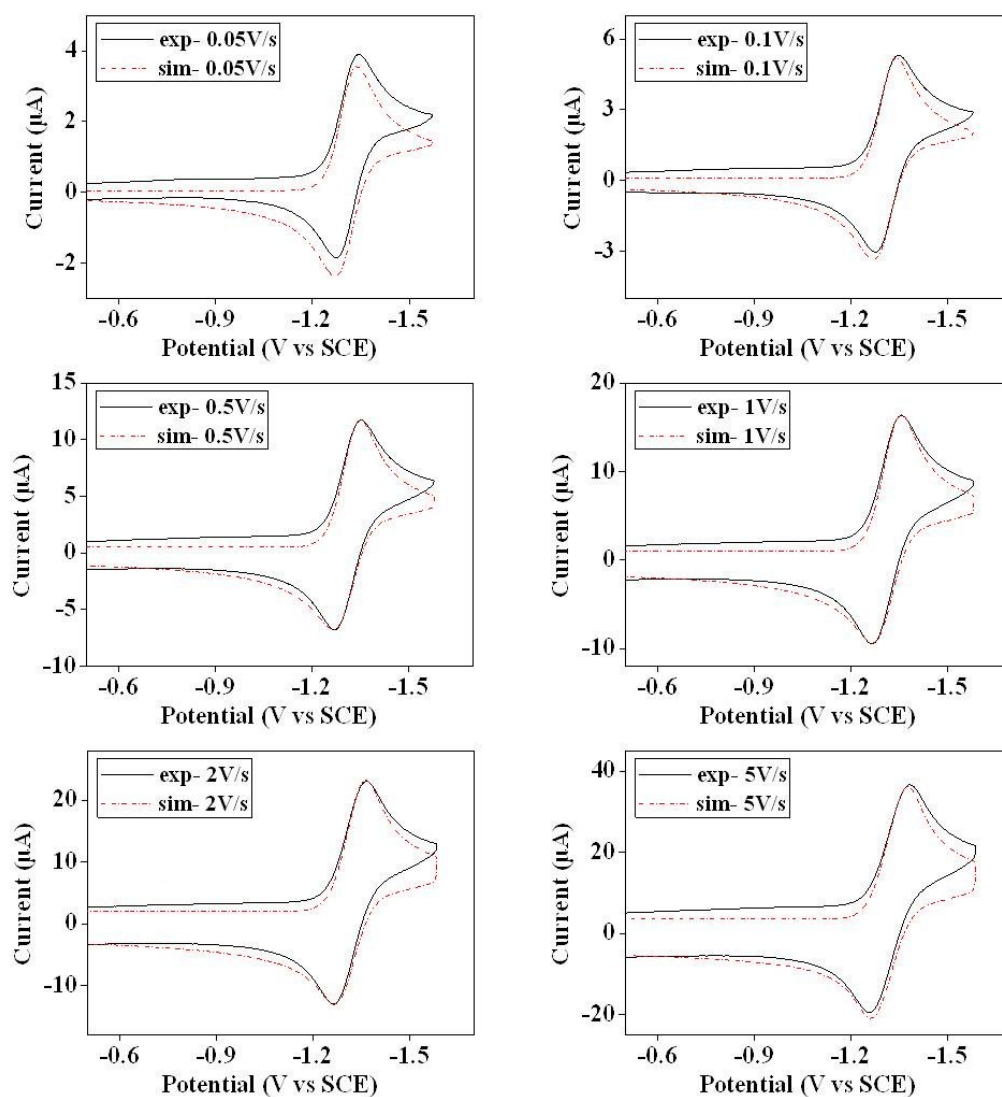


Figure S-18. Comparison between simulated and experimental reduction waves for 1.5 mM TPTZ-TAC2 at different scan rates. The model for these reduction simulations: EC, with $n = 1$, with a heterogeneous rate constant, $\alpha = 0.5$, $k^0 = 1 \times 10^4$ cm/s and a homogeneous forward rate constant, $k_{\text{eq}} = 0.6$, $k_f = 8 \text{ s}^{-1}$. Simulated data: $E^\circ = -1.32$ V vs SCE; Diffusion coefficient: $7.01 \times 10^{-6} \text{ cm}^2/\text{s}$, uncompensated resistance 666Ω , capacitance 1×10^{-6} F. Experimental conditions: solvent: benzene: MeCN (v:v=1:1), supporting electrolyte: 0.1 M TBAPF₆, Pt electrode area 0.027 cm².

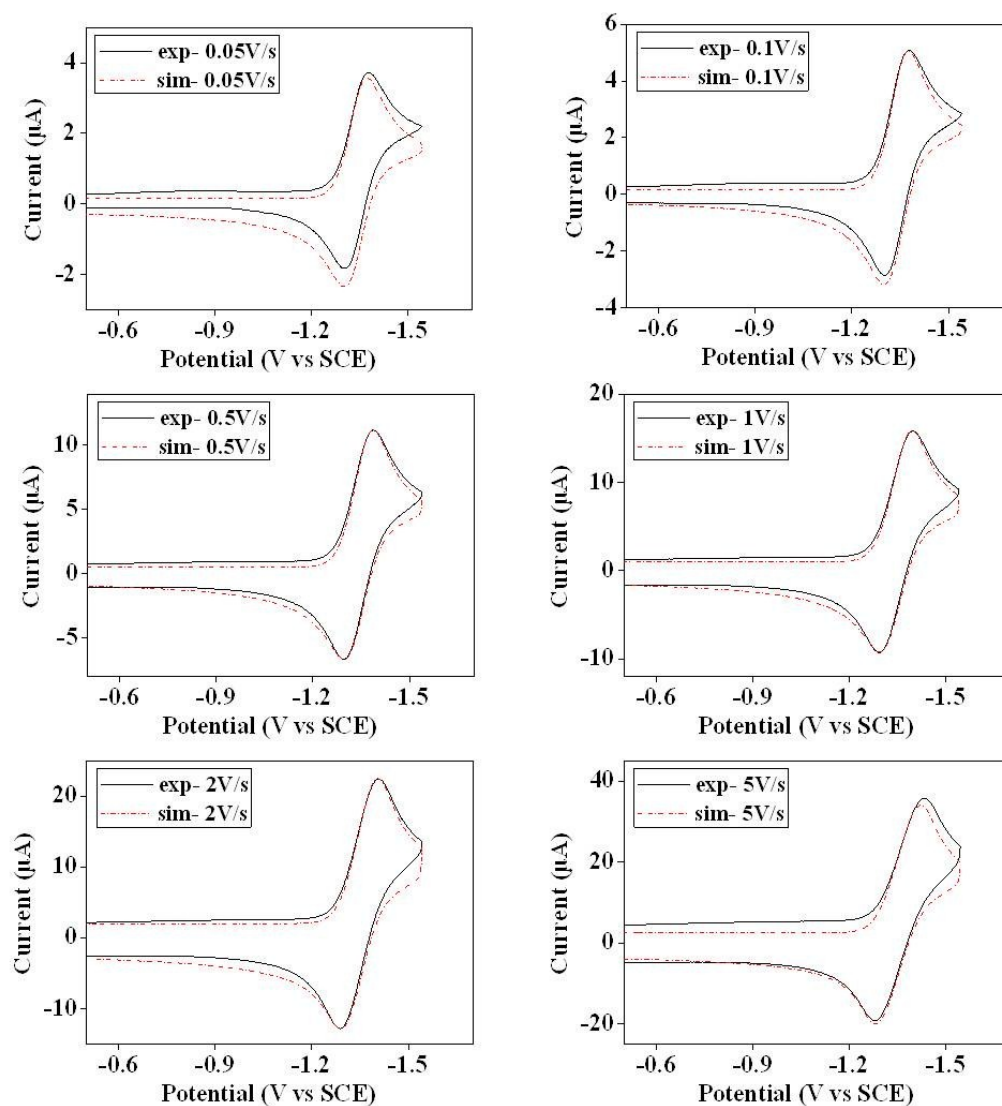


Figure S-19. Comparison between simulated and experimental reduction waves for 1.5 mM TPTZ-TAC3 at different scan rates. The model for these reduction simulations: EC, with $n = 1$, with a heterogeneous rate constant, $\alpha = 0.5$, $k^0 = 1 \times 10^4$ cm/s and a homogeneous forward rate constant, $k_{\text{eq}} = 0.4$, $k_f = 8$ s $^{-1}$. Simulated data: $E^0 = -1.35$ V vs SCE; Diffusion coefficient: 7.00×10^{-6} cm 2 /s, uncompensated resistance 883 Ω , capacitance 3×10^{-6} F. Experimental conditions: solvent: benzene: MeCN (v:v=1:1), supporting electrolyte: 0.1 M TBAPF $_6$, Pt electrode area 0.027 cm 2 .

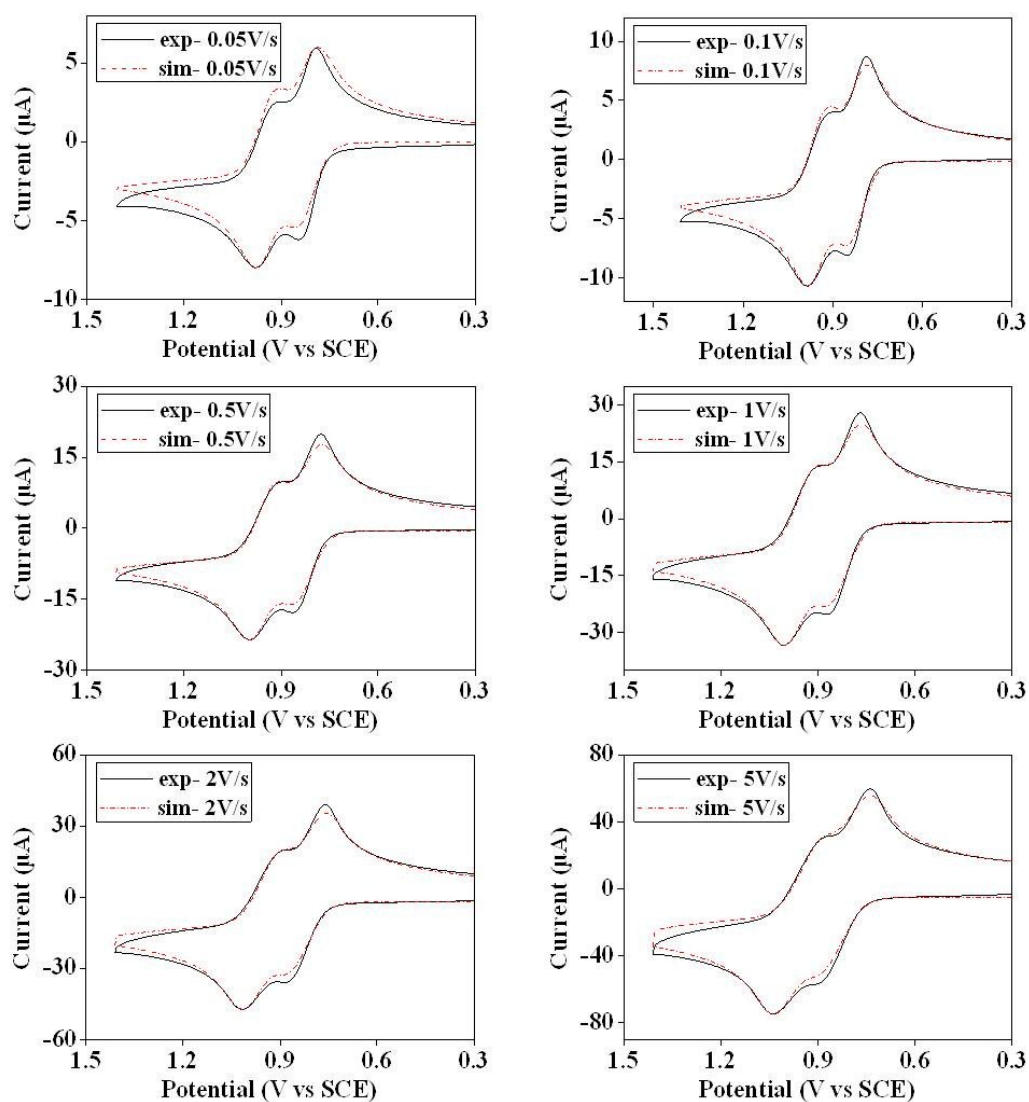


Figure S-20. Comparison between simulated and experimental oxidation waves for 1.5 mM TPTZ-TAC2 at different scan rates. The model for these oxidation simulations: ECE, with $n = 2$, with a heterogeneous rate constant, $\alpha = 0.5$, $k_1^0 = 0.1$ cm/s, $k_2^0 = 0.1$ cm/s. Simulated data: $E_1^0 = 0.82$ V vs SCE, $E_2^0 = 0.95$ V vs SCE; Diffusion coefficient: 7.01×10^{-6} cm²/s, uncompensated resistance 1129 Ω , capacitance 1×10^{-6} F. Experimental conditions: solvent: benzene: MeCN ($v:v=1:1$), supporting electrolyte: 0.1 M TBAPF₆, Pt electrode area 0.027 cm².

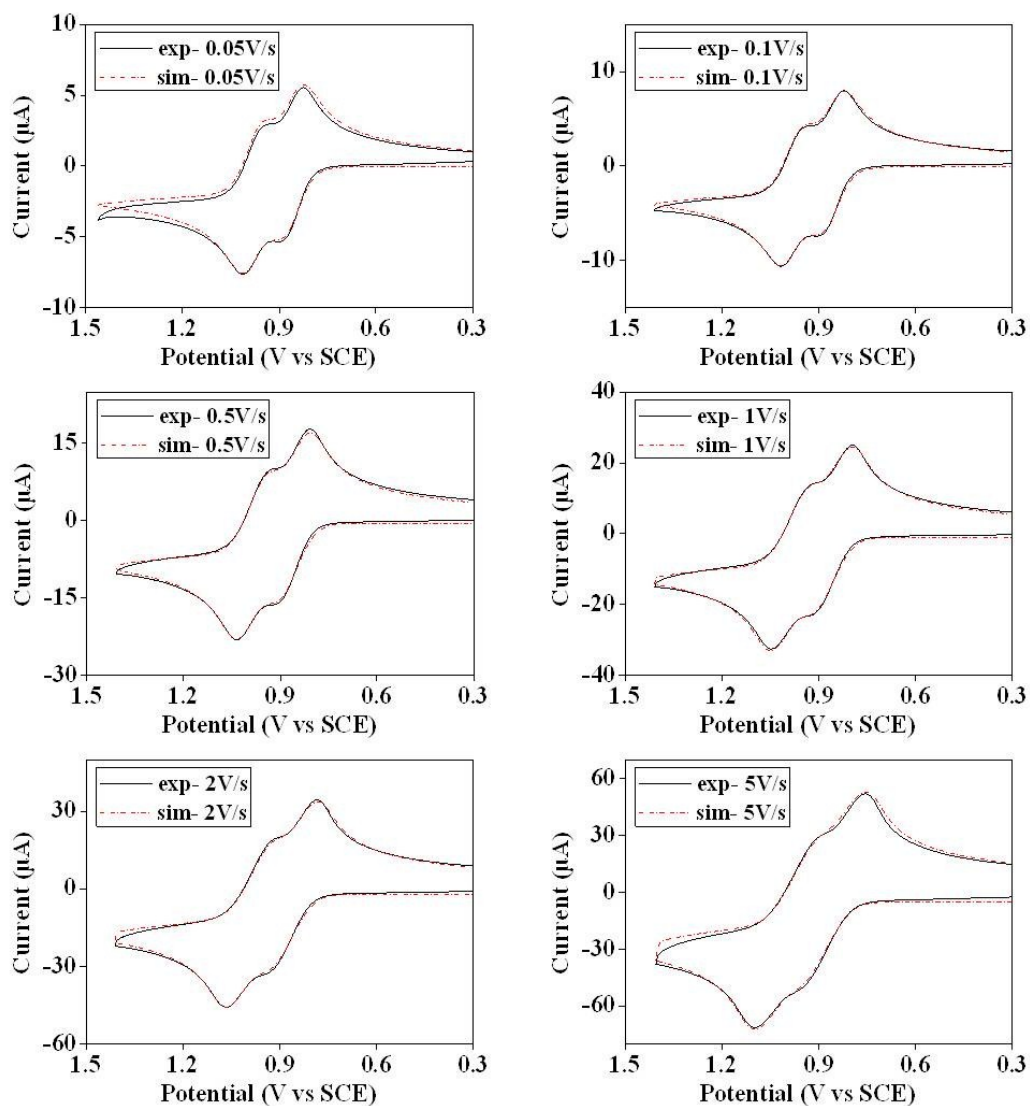


Figure S-21. Comparison between simulated and experimental oxidation waves for 1.5 mM TPTZ-TAC3 at different scan rates. The model for these oxidation simulations: ECE, with $n = 2$, with a heterogeneous rate constant, $\alpha = 0.5$, $k_1^0 = 0.1$ cm/s, $k_2^0 = 0.1$ cm/s. Simulated data: $E_1^0 = 0.86$ V vs SCE, $E_2^0 = 0.97$ V vs SCE; Diffusion coefficient: 7.00×10^{-6} cm²/s, uncompensated resistance 1060 Ω , capacitance 1×10^{-6} F. Experimental conditions: solvent: benzene: MeCN ($v:v=1:1$), supporting electrolyte: 0.1 M TBAPF₆, Pt electrode area 0.027 cm².

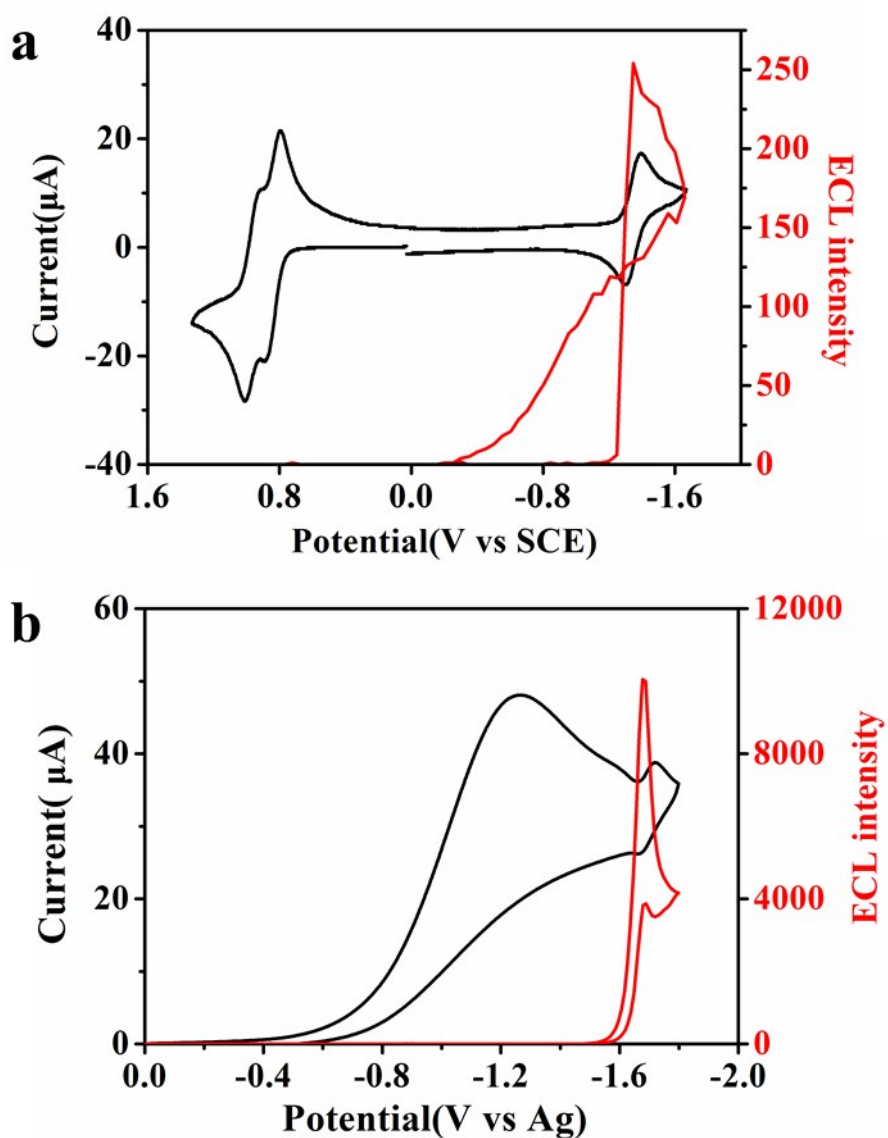


Figure S-22. ECL (red) and CV (black) simultaneous measurements for 1.5 mM TPTZ-TAC1 in the absence (a) and in the presence (b) of 10 mM benzoyl peroxide (BPO), Experimental conditions: solvent: benzene: MeCN ($v:v=1:1$), supporting electrolyte: 0.1 M TBAPF₆, negative high-voltage: 600 V, Pt electrode area 0.027 cm².

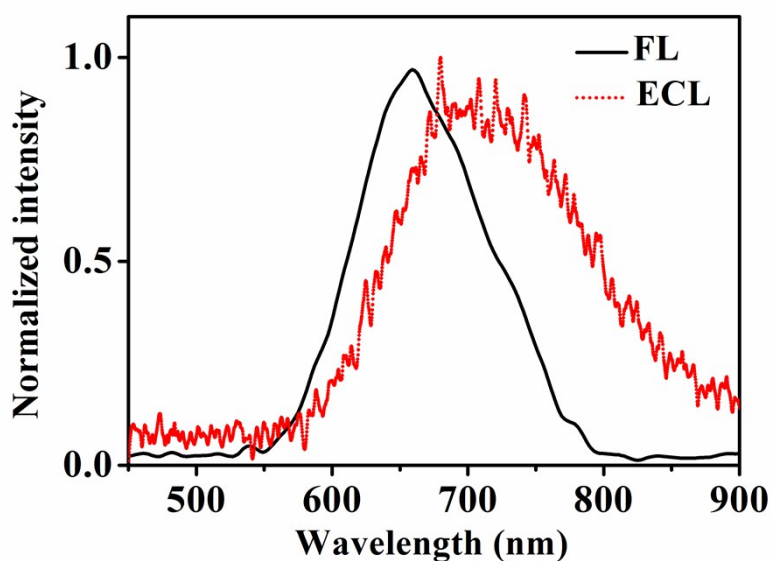


Figure S-23. Normalized fluorescence (solid, black) and ECL (short dot, red) spectra of TPTZ-TAC1 in benzene: MeCN ($v:v=1:1$) solution; ECL conditions were same as Figure 5. The concentration of TPTC-TAC1 is 1×10^{-3} M for fluorescence and ECL spectrum. Slit width is 5 nm for fluorescence and 20 nm for ECL spectrum.

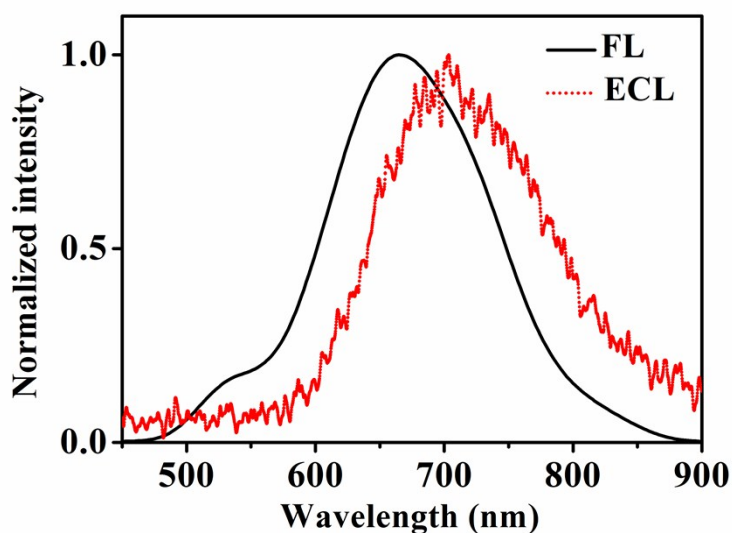


Figure S-24. Normalized fluorescence (solid, black) and ECL (short dot, red) spectra of TPTZ-TAC2 in benzene: MeCN ($v:v=1:1$) solution; ECL conditions were same as Figure 5. The concentration of TPTC-TAC2 is 1×10^{-3} M for fluorescence and ECL spectrum.

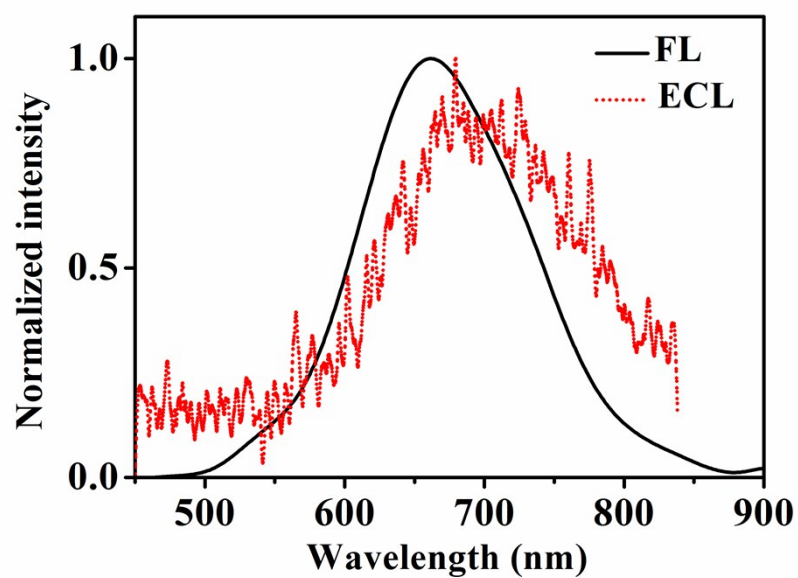


Figure S-25. Normalized fluorescence (solid, black) and ECL (short dot, red) spectra of TPTZ-TAC3 in benzene: MeCN ($v:v=1:1$) solution; ECL conditions were same as Figure 5. The concentration of TPTC-TAC3 is 1×10^{-3} M for fluorescence and 1×10^{-3} M for ECL spectrum.